JPn Neuroscience

The Journal of Physiology

J Physiol 591.4 (2013) pp 973–983

RAPID REPORT

Hyperpolarization of resting membrane potential causes retraction of spontaneous Ca_i^{2+} transients during mouse embryonic circuit development

Hirofumi Watari[1], Amanda J. Tose[2] and Martha M. Bosma[1,2]

[1]*Graduate Program in Neurobiology & Behavior and* [2]*Department of Biology, Box 351800, University of Washington, Seattle, WA 98195, USA*

Key points

- A wave of electrical activity occurs in the developing brain for a certain period of time before sensory, motor and cognitive functions mature.
- This electrical activity, or spontaneous activity, originates, spreads, then later retracts and disappears in specific areas of the brain at specific time points, but how it retracts is unknown.
- We report that retraction in the mouse embryonic hindbrain is caused by a reduced excitability in the network of cells. This process can be reversed by bath application of high K^+ solution, which increases excitability.
- This reduced excitability is probably caused by increased number of K^+ pores that are always open in individual cells.
- These results help us understand how the spread of spontaneous activity is regulated and ultimately help us better understand the role of electrical activity during development of the fetal brain.

Abstract Spontaneous activity supports developmental processes in many brain regions during embryogenesis, and the spatial extent and frequency of the spontaneous activity are tightly regulated by stage. In the developing mouse hindbrain, spontaneous activity propagates widely and the waves can cover the entire hindbrain at E11.5. The activity then retracts to waves that are spatially restricted to the rostral midline at E13.5, before disappearing altogether by E15.5. However, the mechanism of retraction is unknown. We studied passive membrane properties of cells that are spatiotemporally relevant to the pattern of retraction in mouse embryonic hindbrain using whole-cell patch clamp and Ca_i^{2+} imaging techniques. We find that membrane excitability progressively decreases due to hyperpolarization of resting membrane potential and increased resting conductance density between E11.5 and E15.5, in a spatiotemporal pattern correlated with the retraction sequence. Retraction can be acutely reversed by membrane depolarization at E15.5, and the induced events propagate similarly to spontaneous activity at earlier stages, though without involving gap junctional coupling. Manipulation of $[K^+]_o$ or $[Cl^-]_o$ reveals that membrane potential follows E_K more closely than E_{Cl}, suggesting a dominant role for K^+ conductance in the membrane hyperpolarization. Reducing membrane excitability by hyperpolarization of the resting membrane potential and increasing resting conductance are effective mechanisms to desynchronize spontaneous activity in a spatiotemporal manner, while allowing information processing to occur at the synaptic and cellular level.

DOI: 10.1113/jphysiol.2012.244954

(Received 13 September 2012; accepted after revision 15 November 2012; first published online 19 November 2012)
Corresponding author M. M. Bosma: Department of Biology, Box 351800, University of Washington, Seattle, WA 98195, USA. Email: martibee@uw.edu

Abbreviations E, embryonic day; E_{ion}, Nernst potential for ion; InZ, initiation zone; r, rhombomere; K_{2P}, two-pore domain potassium.

Introduction

Spontaneous electrical activity supports activity-dependent neuronal circuit formation (Moody & Bosma, 2005) by varying $[Ca^{2+}]_i$ in a temporally specific manner during embryogenesis, affecting gene expression and resultant phenotypes (Spitzer, 2006). Spontaneous activity is a conserved phenomenon among developing vertebrates and has been shown to occur in rat (Garaschuk *et al.* 2000), mouse (Corlew *et al.* 2004; Hunt *et al.* 2005) and chick (O'Donovan *et al.* 1998; Hughes *et al.* 2009; Wang *et al.* 2009) embryonic and neonatal nervous systems. Spontaneous activity occurs in many regions of the developing nervous system including neocortex (Garaschuk *et al.* 2000; Corlew *et al.* 2004), retina (Meister *et al.* 1991), spinal cord (O'Donovan *et al.* 1998), midbrain (Rockhill *et al.* 2009) and hindbrain (Hunt *et al.* 2005).

The spatial extent and frequency of spontaneous activity appear to be regulated precisely in a temporal fashion (Hunt *et al.* 2006*b*; Conhaim *et al.* 2011), most probably to regulate sequences of gene expression. In the mouse hindbrain, the midline and lateral cells experience repetitive events involving a rise in $[Ca^{2+}]_i$ at E11.5 (Gust *et al.* 2003) driven by spontaneous membrane depolarization (Moruzzi *et al.* 2009), and spontaneous activity can spread to cover the entire hindbrain (Hunt *et al.* 2006*b*). However, this coverage area shrinks during development as the spread of spontaneous activity retracts, first from lateral regions at E12.5, then, between E13.5 and E14.5, towards the initiation zone (InZ), a defined origin at the midline of former rhombomere (r)2 (Moruzzi *et al.* 2009). By E13.5, the frequency of spontaneous activity decreases, and the spontaneous activity disappears altogether from the hindbrain by E14.5 (Hunt *et al.* 2006*b*; Bosma, 2010).

As each spontaneous depolarizing event causes an influx of calcium (Moruzzi *et al.* 2009), which can modulate cellular processes including gene expression, the timing and consequence of spontaneous activity retraction and ultimate disappearance probably has an impact on neuronal circuit formation during embryogenesis. How spontaneous activity retracts is still unknown. Here, we provide evidence that hyperpolarization of resting membrane potential and increased resting conductance may underlie the retraction of spontaneous activity in the embryonic mouse hindbrain. The resulting reduction in membrane excitability is an effective mechanism to desynchronize spontaneous activity in a spatiotemporal manner, while allowing information processing to occur at the synaptic and cellular level.

Methods

Animals

Timed-pregnant Swiss/Webster mice were either bred in the lab or purchased from Harlan Laboratories (Livermore, CA, USA). The animals were killed by CO_2 followed by cervical dislocation. Care for animals and euthanasia procedures were approved by University of Washington Animal Care Committee (IACUC). Embryos at E10.5–E15.5 were kept in ACSF, containing (in mM): 119 NaCl, 2.5 KCl, 1.3 $MgCl_2$, 2.5 $CaCl_2$, 1 NaH_2PO_4, 26 $NaHCO_3$, 30 glucose, and bubbled in carbogen (95% O_2, 5% CO_2). For high $[K^+]_o$ experiments, an equivalent molar concentration of NaCl was replaced by KCl. We used 12–15 mM $[K^+]_o$ for these experiments. For low $[Cl^-]_o$ experiments, an equivalent molar concentration of NaCl was replaced with sodium gluconate. All external solutions have osmolarity of 316 ± 1 mosmol l^{-1}. Hindbrains were dissected as previously described (Moruzzi *et al.* 2009). All experiments were done at approximately 23°C.

Calcium imaging

Hindbrains were removed and incubated in oxygenated ACSF for 15 min with the $[Ca^{2+}]_i$ indicators fluo-4 or fluo-8 and pluronic F-127. The change in fluorescence was measured in up to 48 regions of interest (ROIs) in the former r2 or r5 regions using MetaFluor (Universal Imaging/Molecular Devices, Downington, PA, USA), with an image capture rate of 1 Hz or 2.43 Hz. The perfusion rate of the oxygenated ACSF was maintained at 1 ± 0.3 ml min^{-1} during recording. Meclofenamic acid was from Sigma-Aldrich Co. (St Louis, MO, USA). Mefloquine was from Tocris Bioscience (Ellisville, MO, USA). The calcium imaging data were visualized and analysed in Igor Pro 6 (Wavemetrics, Inc., Lake Oswego, OR, USA) and ImageJ (National Institutes of Health, Bethesda, MD, USA).

Electrophysiology

Whole-cell patch clamp recording was performed on cells from three hindbrain regions: at the midline in the former r2 where >90% of spontaneous activity events originate (InZ); in lateral cells 200 μm from the midline of the InZ; and midline cells in the former r5, where events rarely initiate. Pipettes of resistance 2.5–5 MΩ approached from the ventricular side in the open-book configuration, as described previously (Moruzzi *et al.* 2009). Internal solution contained (in mM): 100 potassium gluconate, 15 KCl, 1 EGTA, 5 $MgCl_2$, 40 Hepes, 3 Na-ATP and 0.3 Na-GTP (adapted from Mooney *et al.* 1996; Moruzzi *et al.* 2009). pH was titrated to 7.25 by addition of NaOH. Osmolarity was adjusted to 328 ± 2 mosmol l^{-1} by addition of sucrose. For these solutions, $E_K = -97.4$ mV and $E_{Cl} = -42.2$ mV (Hille, 2001). The perfusion rate of the oxygenated ACSF was maintained at 1 ± 0.3 ml min^{-1} during recording. Data were acquired using an Axopatch-1D or Axopatch 200B amplifier with pCLAMP 8 (Molecular Devices, LLC. Sunnyvale, CA, USA). Signals were low-pass Bessel filtered with cut-off frequencies of 2 or 5 kHz. Signals were digitized at 5–10 kHz. In the ramp voltage clamp experiment, first the voltage was stepped from the holding potential of −60 mV to +80 mV for 150 ms to inactivate inward current response, then ramped from +80 mV to −100 mV at the rate of −233 mV s^{-1}. This rate is equivalent to the protocol used previously (Moruzzi *et al.* 2009). The current clamp traces were decimated offline without smoothing by a factor of 10 to an equivalent of 500 Hz sampling frequency to reduce the baseline noise that was introduced due to oversampling; the decimation effectively reduced baseline noise without affecting the waveform of the events. Liquid junction potential of −6.3 mV caused by the perfusion of low $[Cl^-]_o$ ACSF was calculated in Clampex (Molecular Devices) and was corrected for offline. All analyses were done using Igor Pro 6.

Results

Spontaneous activity retracts and disappears between E11.5 and E15.5

In the developing mouse embryonic hindbrain, spontaneous $[Ca^{2+}]_i$ transients are driven by spontaneous membrane depolarization (Moruzzi *et al.* 2009), which opens $Ca_v3.3$ channels mediating T-type Ca^{2+} currents and causes a rise in $[Ca^{2+}]_i$ (Hughes *et al.* 2009; Moruzzi *et al.* 2009). Most Ca^{2+} events initiate in the midline of former r2 (the initiation zone, or InZ) at E11.5 (Fig. 1*A*, 1.6 s) and occur with a frequency of 3.2 ± 0.2 min^{-1} (Hunt *et al.* 2006*b*). These events propagate rostrally and caudally along the midline of the hindbrain (Fig. 1*B* and *D*, top left; Fig. 1*C*, left, dark red) and, with lower intensity and frequency, into the lateral regions (Hunt *et al.* 2005) (Fig. 1*B* and *D*, bottom left; Fig. 1*C*, left, light red). The propagation requires both 5-$HT_{2A,C}$ receptor activation and gap junctional coupling, as judged by the block of activity by ketanserin, spiperone and gap junction blockers (Hunt *et al.* 2005, 2006*a*). Over the course of development, at E13.5, spontaneous activity retracts towards the InZ (Fig. 1*B*, *C* and *D*, middle; Hunt *et al.* 2006*b*). Waves in the lateral regions disappear (Fig. 1*D*, bottom middle) and do not propagate as caudally as they do in the midline of E11.5 (Fig. 1*D*, top middle). All events are extinguished at E15.5 (Fig. 1*B*, *C* and *D*, right).

Membrane hyperpolarizes from E11.5 to E15.5

We asked whether retraction is caused by spatially regulated changes in intrinsic membrane properties. We performed whole-cell patch clamp on cells from three sites that are spatially and temporally relevant to the pattern of retraction: the InZ (r2 midline), where most events originate and where events persist into late stages (Fig. 2*A*, grey); lateral cells 200 μm from the InZ, where events retract first (Fig. 2*A*, red); and midline cells in the former r5, where events rarely initiate but where events propagate until E13.5 (Hunt *et al.* 2006*b*) (Fig. 2*A*, blue).

Current clamp recordings reveal that cells at all three sites have equivalent resting membrane potentials at E10.5 (Fig. 2*C*). Then, the membrane hyperpolarizes progressively between E11.5 and E15.5 (Fig. 2*B* and *C*). The hyperpolarization occurs first in lateral cells (red traces; -52.1 ± 2.1 mV at E11.5, $n = 14$ *vs.* -76.4 ± 1.4 mV at E15.5, $n = 20$; $^{***}P < 0.001$). Subsequently, midline cells in the caudal sites hyperpolarize and have the largest change of up to 50 mV (blue traces; -32.8 ± 2.7 mV at E11.5, $n = 19$ *vs.* -75.8 ± 1.7 mV at E15.5, $n = 15$; $^{***}P < 0.001$). The cells of the InZ remain depolarized until E13.5. They then hyperpolarize, and to the least extent (grey traces; -40.2 ± 3.6 mV at E13.5, $n = 15$ *vs.* -62.6 ± 2.0 mV at E15.5, $n = 15$; $^{**}P < 0.01$). The pattern of hyperpolarization mirrors the spatial pattern of retraction of spontaneous activity (Hunt *et al.* 2006*b*) (Fig. 1*C*). We next investigated the mechanism of the hyperpolarization.

Resting conductance density increases from E11.5 to E15.5

We have previously shown that lateral cells have a significantly higher resting conductance than midline cells at E11.5 (Moruzzi *et al.* 2009), and our current data confirm this difference (Fig. 2*D* and *E*, red *vs.* grey traces at E11.5). We measured current–voltage (*I–V*) relations using a voltage ramp protocol at E10.5–E15.5.

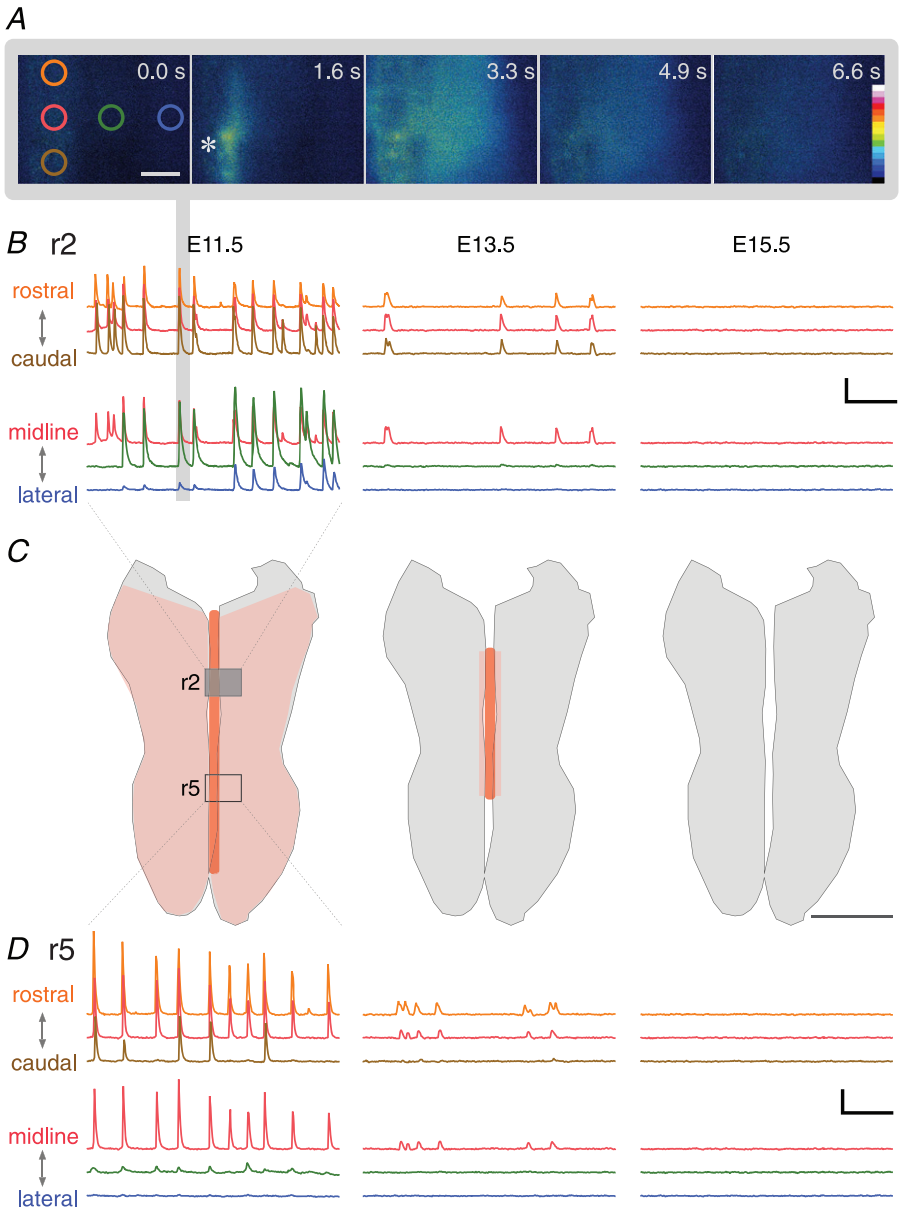

Figure 1. Spontaneous activity retracts and disappears between E11.5 and E15.5
A, frames of images show initiation and propagation of an event at E11.5. The images were pseudocoloured to show a gradient of intensities in the fluorescence (white, high intensity; black, low intensity). The coloured circles indicate regions of interest (ROIs, at 0.0 s) positioned along the midline (orange, red, brown) and mediolaterally (red, green, blue) within former rhombomere (r)2. Initiation of an event starts as an increase in fluorescence at 1.6 s (InZ, indicated by *). The event then spreads along the midline axis (1.6, 3.3 and 4.9 s) and then laterally (3.3 and 4.9 s). Scale bar: 100 μm. *B*, representative $[Ca^{2+}]_i$ traces recorded at E11.5 (left), E13.5 (middle) and E15.5 (right) in r2, showing rostrocaudal (top) and mediolateral (bottom) propagation. Traces are stacked and the colour corresponds to the position of ROIs shown in *A*. The event from the images in *A* is marked with grey vertical bar. Scale bar (applies to all graphs): 5 $\Delta F/F$, 1 min. *C*, spread of spontaneous activity is greatest at E11.5 (left) where it can cover the entire surface of the hindbrain. Intensity of Ca^{2+} signal is greater at the midline (dark red) compared with the lateral regions (light red). The region of Ca^{2+} imaging shown in *A* and *B* is indicated by grey rectangle, marked 'r2'. The region of Ca^{2+} imaging shown in *D* is indicated by open rectangle, marked 'r5' (left). The propagation retracts laterally and medially at E13.5 (middle). Spontaneous activity disappears by E15.5 (right). Some parts of the figure are adapted and modified from Hunt *et al.* (2006*b*). Scale bar: 1 mm. *D*, representative $[Ca^{2+}]_i$ traces recorded at E11.5 (left), E13.5 (middle) and E15.5 (right) in r5, marked by the open rectangle in *C*, showing rostrocaudal (top) and mediolateral (bottom) propagation. Traces are stacked and the colour corresponds to the position of ROIs shown in *A*. Scale bar (applies to all graphs): 5 $\Delta F/F$, 1 min.

The *I–V* relation is linear between −90 mV and −60 mV, and the slope within this range is used to measure the conductance (Fig. 2*D*). To account for a possible change in cell size across stages, the conductance was normalized to membrane capacitance. In lateral regions, where events propagate with lower $[Ca^{2+}]_i$ intensity, the resting conductance density is significantly higher than the midline cells at E11.5 (Fig. 2*E*; midline r2, grey, $n = 23$ *vs.* lateral r2, red, $n = 13$; $^{***}P < 0.001$). The conductance density of the lateral cells nearly doubles

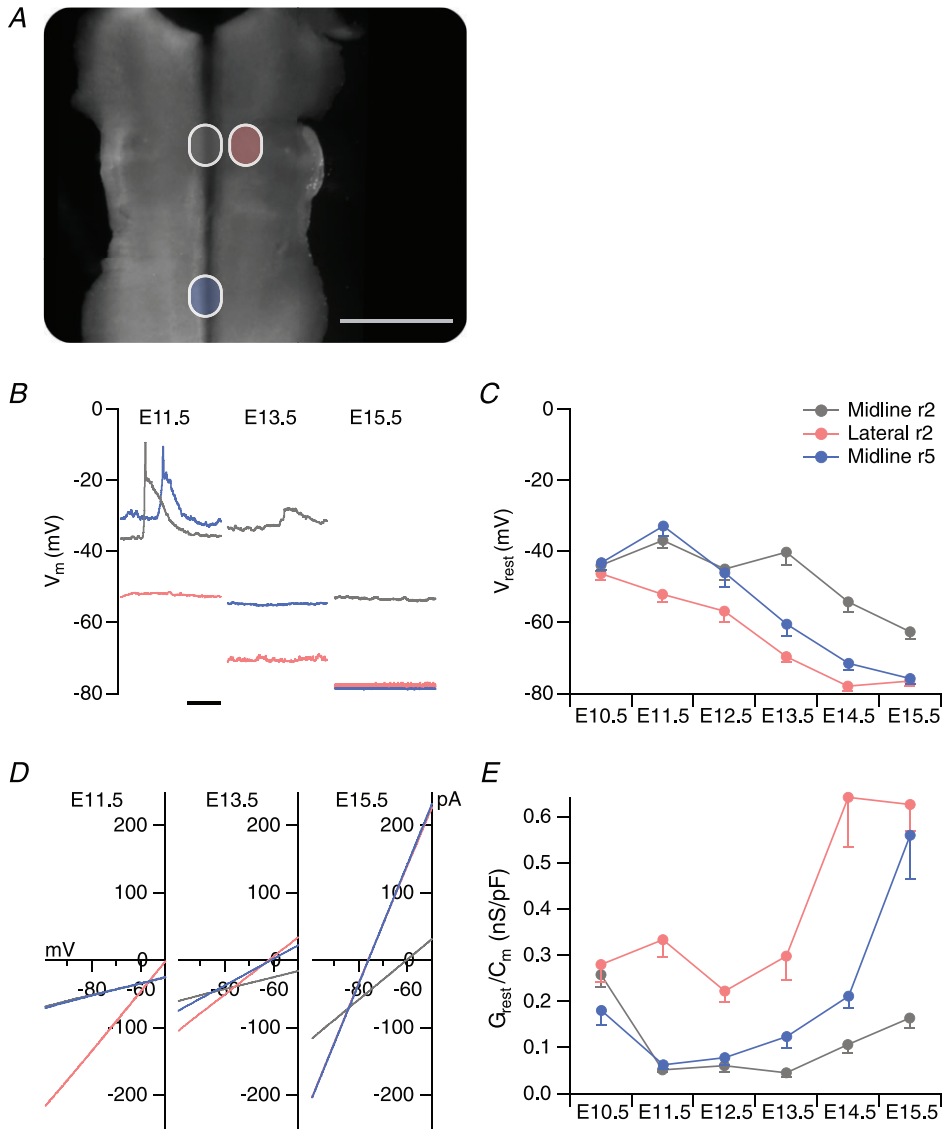

Figure 2. Membrane potential hyperpolarizes from E11.5 to E15.5 with changes in resting conductance density

A, light microscope image of the hindbrain used in electrophysiology experiments. Whole-cell patch clamp was performed on cells in three coloured regions: midline r2 (grey, InZ), lateral r2 (red), midline r5 (blue). Scale bar: 1 mm. *B*, representative membrane potential (V_m) is shown for cells recorded in current clamp at three stages: E11.5 (left), E13.5 (middle) and E15.5 (right). Each coloured trace represents V_m recorded from a cell in the regions as shown in Fig. 2*A*. Scale bar: 1 s. *C*, mean resting membrane potential at each stage from E10.5 to E15.5. *D*, averaged current–voltage (*I–V*) relations after delivering a voltage ramp protocol. At E11.5, the resultant currents from averaged midline r2 and midline r5 cells completely overlap; at E15.5, the currents from midline r5 and lateral r2 overlap. Note the progressive hyperpolarization of the zero-current potential, corresponding to the shift in V_{rest}. *E*, mean resting conductance measured as a slope of the *I–V* relations in *D*, normalized for membrane capacitance. In *C* and *E*, the negative bar represents SEM and $n > 13$ at each stage and location. In all panels, colour of the trace corresponds to regions defined in *A*.

between E13.5 and E14.5 ($n = 14$ and $n = 15$, respectively; $^{**}P < 0.01$) and it remains high at E15.5 ($n = 20$; Fig. 2*E*, red). The midline cells in r5 display the most striking change over time (Fig. 2*E*, blue). The resting conductance density increases by nine-fold in just 4 days starting at E11.5 (E11.5, $n = 19$ *vs.* E15.5, $n = 15$; $^{***}P < 0.001$), and matches the conductance density of the lateral cells by E15.5. Lastly, the cells in the InZ region show the most modest increase in conductance density of the three regions recorded (Fig. 2*E*, grey). The resting conductance density doubles between E13.5 and E14.5 ($n = 22$ and $n = 32$, respectively), the point in time after which the spontaneous activity ceases to be recorded. In summary, the resting conductance density increases by as much as nine-fold between E11.5 and E15.5, and the greatest change occurs at the sites away from the InZ. Both the resting membrane potential and resting conductance density in the InZ do not change between E11.5 and E13.5, allowing initiation of spontaneous activity. The increase in resting conductance density indicates an increase in the density of resting channels, which may contribute to the hyperpolarization of the membrane potential reported above; the selectivity of these channels will be discussed below.

Retraction can be reversed by membrane depolarization at E15.5

Our data demonstrate that progressive hyperpolarization parallels retraction of spontaneous activity between E11.5 and E15.5. If this hyperpolarization causes retraction of spontaneous activity, then acute membrane depolarization should induce events in regions that have undergone retraction. To test this, we increased $[K^+]_o$ to depolarize the membrane at E15.5. We performed whole-cell patch clamp in the midline cells of r5, where the greatest change in the resting membrane potential and resting conductance was observed between E11.5 and E15.5 (Fig. 2*D* and *E*). When $[K^+]_o$ was increased from 2.5 mM to 12–14 mM, the membrane potential of the r5 midline cells of previously quiescent E15.5 hindbrains depolarized from -69.8 ± 2.2 to -49 ± 1.2 mV ($n = 23$, $^{***}P < 0.001$), depolarizing the membrane so that the resultant resting membrane potential was closer to where it was at E12.5–E13.5, and events were induced (Fig. 3*A*). Frequency of events increased from zero to a mean of 1.8 ± 0.4 events min^{-1} ($n = 6$; Fig. 3*B*). A significant change in membrane potential of 17.3 ± 2.4 mV occurred with acute application of 12 mM $[K^+]_o$ ACSF at E15.5 ($n = 8$; Fig. 3*C*, filled circles). A corresponding change of 9.6 ± 2.3 mV was significantly smaller at E11.5 ($n = 8$; Fig. 3*C*, open circles). These experiments show that the mechanisms that support propagation do not disappear during retraction, but are simply suppressed by hyperpolarization.

To test the role of Cl^- conductance in the hyperpolarization, we set E_{Cl} to more positive potentials, and asked if the membrane potential followed E_{Cl}. When $[Cl^-]_o$ was decreased from 129.1 to 39.1 mM (setting E_{Cl} from -41.9 to -11.4 mV), the membrane potential hyperpolarized by -14.6 ± 5.1 mV at E11.5 ($n = 6$) and by -9.3 ± 1.6 mV at E15.5 ($n = 7$) (Fig. 3*D* and *E*). At both stages, the membrane potential moved away from the E_{Cl} set by the low $[Cl^-]_o$ ACSF. Whereas the high $[K^+]_o$ ACSF moved the membrane potential towards both E_K and E_{Cl} (Fig. 3*F*, left), the low $[Cl^-]_o$ ACSF moved it towards E_K but away from E_{Cl} at E15.5 (Fig. 3*F*, right). These results suggest that the increased conductance may be due to an upregulation of K^+-permeable resting ion channels, while little Cl^- conductance is involved in the membrane hyperpolarization.

Serotonin (5-$HT_{2A,C}$) receptor activation is required for spontaneous activity at early stages indicated by the fact that ketanserin blocks events at E11.5 (Hunt *et al.* 2005) and at E13.5 (Hunt *et al.* 2006*a*). However, acute bath application of either 100–500 μM 5-HT ($n = 2$) or 0.5–10 μM fluoxetine ($n = 2$) failed to evoke events at E15.5 (data not shown), suggesting that a decrease in 5-HT receptor function alone does not cause retraction. In contrast, acute bath application of 2 μM AMPA, which is known to have a modulatory effect on frequency of spontaneous activity at E13.5 but not at E11.5 (Hunt *et al.* 2006*a*), can evoke propagating events along the midline axis at E14.5–E15.5 ($n = 5$, data not shown). These results suggest that the underlying mechanism of retraction is not dependent on loss of 5-HT receptor function, and the change in receptor phenotype that happens during retraction is supportive of propagation but not causative to the retraction itself.

Induced events propagate similarly to spontaneous activity

Our whole-cell patch clamp experiment showed that, at E15.5, high $[K^+]_o$ ACSF induced events in individual cells in regions where spontaneous activity has already undergone retraction. We next investigated the spatial extent of the induced events using Ca^{2+} imaging. The events induced by high $[K^+]_o$ ACSF propagate along the midline axis at E15.5 (Fig. 4*A*, top), with restricted propagation laterally (Fig. 4*A*, bottom left), similarly to the way spontaneous activity propagates at earlier stages. The induced events propagate through the midline of both r2 (Fig. 4*A*, left) and, notably, r5 (Fig. 4*A*, right), where propagation terminates caudally (Fig. 1*D*, top middle) and resting membrane hyperpolarizes most robustly (Fig. 2*C*, blue trace). This suggests that mechanisms that support

propagation may still be present in the quiescent E15.5 hindbrain. Propagation of spontaneous activity has been reported to involve gap junctional coupling in developing retina and neocortex (Roerig & Feller, 2000). Likewise, it is known that propagation requires gap junctional coupling at earlier stages in the hindbrain (Hunt *et al.* 2006*a*). To test for a functional role of gap junction coupling at E15.5, we bath applied gap junction blockers and probed for events with high $[K^+]_o$ ACSF in the InZ region. Whereas the events at E11.5 disappear with bath application of 200 μM meclofenamic acid ($n = 8$, data not shown) or 100 μM mefloquine ($n = 5$; also see Moruzzi *et al.* 2009), the high $[K^+]_o$-induced events are still capable of propagating in the presence of these gap junction blockers at E15.5 (Fig. 4*B*, meclofenamic acid, 4 of 4; mefloquine, 5 of 6, data not shown). Events during the second high $[K^+]_o$ application have smaller amplitudes due to photobleaching ($n = 3$ control experiments; data not shown). These results suggest that acute membrane depolarization can increase spatial extent of the induced events and, at E15.5, such event propagation no longer requires gap junctional coupling.

Discussion

Activity-dependent gene expression has been proposed as a mechanism that is involved in neuronal circuit formation (Flavell & Greenberg, 2008). The key component to this hypothesis is the calcium influx, which can modulate many cellular processes including gene expression. Spontaneous activity during embryogenesis can support this function by regulating $[Ca^{2+}]_i$ both temporally and spatially, and may therefore orchestrate many developmental processes including proliferation, migration, differentiation, transmitter phenotype, axonal guidance, synaptogenesis and ion channel expression (Moody & Bosma, 2005; Spitzer, 2006; Hanson *et al.* 2008).

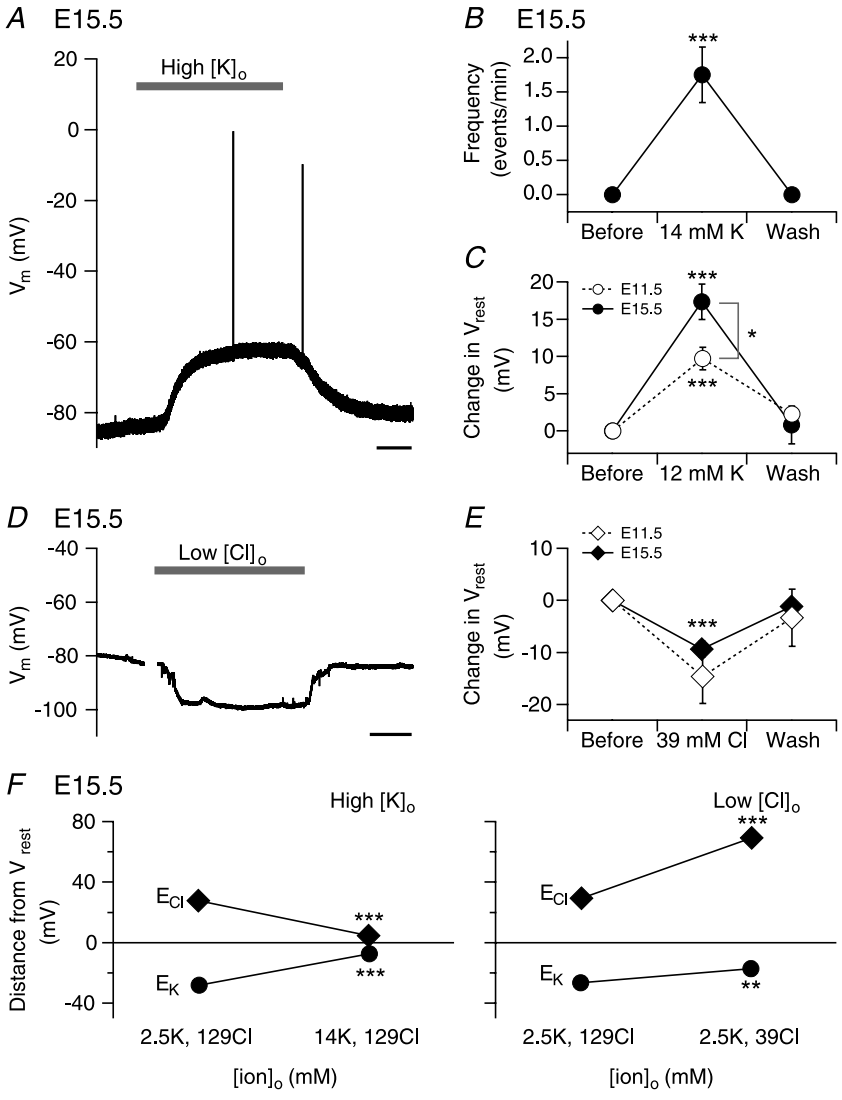

Figure 3. Cessation of events can be reversed by membrane depolarization at E15.5
A, representative trace recorded from cells in midline r5 shows response to acute bath application of high $[K^+]_o$ ACSF. Scale bar: 2 min. *B*, change in event frequency for cells in midline r5 during bath application and after washout of high $[K^+]_o$ ACSF. *C*, change in V_{rest} recorded from cells in midline r5 during bath application and after washout of high $[K^+]_o$ ACSF. *D*, representative trace recorded from cells in midline r5 shows hyperpolarizing response to acute bath application of low $[Cl^-]_o$ ACSF. Scale bar: 2 min. *E*, change in V_{rest} recorded from cells in midline r5 during bath application and after washout of low $[Cl^-]_o$ ACSF. *F*, distance in mV between the Nernst potentials (E_K, circles; E_{Cl}, diamonds) and the V_{rest} before and during high $[K^+]_o$ ACSF (left) or low $[Cl^-]_o$ ACSF (right). The effect of liquid junction potential (−6.3 mV) caused by the application of low $[Cl^-]_o$ is corrected for in *E* and *F* but not in *D*. In *B*, *C*, *E* and *F*, the bars represent SEM.

Several models describe spatiotemporal regulation of spontaneous activity (Butts *et al.* 1999; Godfrey & Swindale, 2007; Hennig *et al.* 2009). Spatiotemporal properties of retinal waves are influenced by a variable fraction of recruitable cells in the neighbouring area, and the propagation stops when the fraction is small (Butts *et al.* 1999). In this model, the recruitable cells are defined by an intrinsic refractory period, so each cell can theoretically switch from being recruitable to non-recruitable, and *vice versa*, within minutes if not seconds. Spontaneous activity retraction in the hindbrain, however, occurs over hours and days, so the recruitable cells must be defined by properties other than the refractory period.

We have found a novel mechanism of spontaneous activity retraction. Between E11.5 and E15.5, the hindbrain cells exhibit a decrease in the membrane excitability measured by hyperpolarization of the resting membrane potential and increase in resting conductance (Fig. 2). At a stage before widespread waves of spontaneous activity occur, E10.5 (Gust *et al.* 2003; unpublished observation, authors), cells at all recorded sites have similar resting membrane potentials (Fig. 2*C*). Midline cells subsequently depolarize slightly, while lateral cells begin the process of gradual hyperpolarization. Then, the midline cells hyperpolarize, first at sites away from the InZ, then the InZ itself, defining the end of the window of spontaneous activity. The spatiotemporal pattern of this change (Fig. 5) matches the known spatiotemporal pattern of retraction (Hunt *et al.* 2006*b*) (Fig. 1*C*). For example, the propagation of spontaneous activity terminates caudally in r4–r5 at E13.5 (Fig. 1*D*, top middle), and these Ca^{2+} imaging data correlate well with the electrophysiology data that shows resting membrane hyperpolarization and increase in resting conductance density in r5 (Fig. 2*C* and *E*,

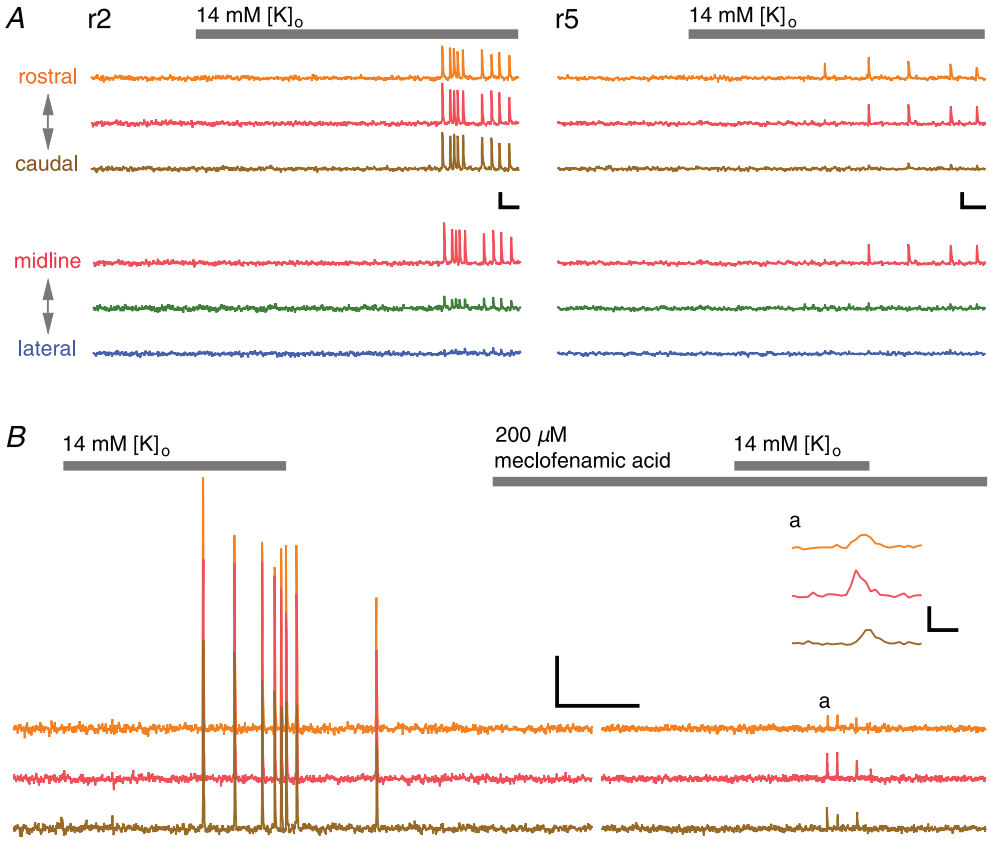

Figure 4. Evoked events propagate independently of gap junction coupling in E15.5
A, representative Δ*F*/*F* fluorescence traces recorded at r2 (left) and r5 (right) show propagation of Ca^{2+} events along the midline axis (top) with restricted lateral spread (bottom left), caused by acute bath application of high $[K^+]_o$ ACSF. Separate experiments are shown for each region. The Ca^{2+} imaging in midline r5 (right) is recorded from the same location where electrophysiology was performed in Fig. 3. Scale bar (all graphs): 1 Δ*F*/*F*, 1 min. *B*, representative Δ*F*/*F* fluorescence traces recorded at midline r2 show propagation of Ca^{2+} events along the midline caused by application of high $[K^+]_o$ ACSF in the absence and in the presence of meclofenamic acid at E15.5. Inset a, representative Δ*F*/*F* fluorescence trace corresponding to label a in the main trace. Inactivity during drug application (14 min) is omitted from the trace. Scale bar: 2 Δ*F*/*F*, 5 min; 1 Δ*F*/*F*, 6 s (inset). The amplitudes of events look smaller during the second high $[K^+]_o$ probe because of photobleaching. In all panels, colour of the traces indicate ROIs as shown in Fig. 1*A*.

blue traces). The retraction can be acutely reversed by membrane depolarization induced by application of high $[K^+]_o$ ACSF (Figs 3 and 4). Taken together, retraction is probably caused by the changes in the passive membrane properties of the cells.

Possible mechanism of membrane hyperpolarization

There are several possible mechanisms for hyperpolarization to occur. First, the concentration gradient for ions may have changed. In the mouse spinal cord–hindbrain preparation, the disappearance of similarly synchronized electrical waves (which are different in origin and mechanism from those recorded in this study) are attributed to changes in the chloride concentration gradient (Momose-Sato *et al.* 2012*a*,*b*). Our experiments argue against contribution of a shift in E_{Cl}. Clearly, hyperpolarization and change in resting conductance density was still observed even when the ion gradients were controlled within the cells recorded under whole-cell patch clamp.

Second, there may be upregulation of a new kind of ion channel that is open at rest. If this was true, we would predict resting conductance to increase. Indeed, this increase correlates both spatially and temporally with the retraction of spontaneous activity (Figs 2 and 5). A combination of both the hyperpolarization and the increased conductance would act to decrease membrane excitability, and this in turn would contribute to the retraction and cessation of the spontaneous activity.

If a new kind of ion channel is expressed, to what ion is it permeable? As the membrane potential hyperpolarizes towards E_K (−97.4 mV) and away from E_{Cl} (−42.2 mV) (Fig. 2*B* and *C*), the channel is most likely to be permeable to K^+ ions. In support of this hypothesis, the membrane potential changed by the high $[K^+]_o$ ACSF followed E_K more closely at E15.5 (Fig. 3*F*). Since the linear *I*–*V* relations follow the Goldman–Hodgkin–Katz equation (Hille, 2001) at negative potentials (Fig. 2*D*), the channels are likely to be open at rest, typical of leak channels. A candidate leak channel, the two-pore domain potassium (K_{2P}) family, fits this description. There are three K_{2P} channel types that appear to be present in the mouse hindbrain at E15.5 based on *in situ* hybridization: TREK-1, TREK-2 and TASK-3 (Aller & Wisden, 2008). A lack of specific pharmacological blockers for these channels makes it difficult to identify the functional presence of these channels.

At E15.5, gap junction blockers failed to prevent propagation of events evoked by high $[K^+]_o$ ACSF (Fig. 4*B*). This suggests that retraction may be caused by reduced gap junctional coupling. While the present study does not fully explore this possibility, we think that changes in gap junctional coupling have a minor role in the retraction. As an example, if gap junctional coupling is reduced, the conductance should decrease. However, we observed just the opposite: there was an increase in the conductance (Fig. 2*D* and *E*). Even if gap junctional coupling was decreased, the corresponding decrease in the conductance may be masked by the increase in K^+ conductance, which is dominant.

Possible role for spontaneous activity retraction

Spontaneous activity plays an important role in the formation of neuronal circuits, and it has been reported to affect proliferation, migration, differentiation, axonal guidance, synaptogenesis and ion channel expression (Moody & Bosma, 2005; Spitzer, 2006; Hanson *et al.* 2008). The retraction and cessation of activity may have several crucial consequences on circuit development. First, it is possible that spontaneous activity regulates cellular proliferation or migration. Between E10.5 and E15.5, the hindbrain changes thickness of the tissue from the ventricular zone to the pial surface, indicative of continued proliferation during periods at which the spontaneous activity is present (data not shown). Perhaps this process requires calcium influx, as has been shown to occur in developing neocortex (Weissman *et al.* 2004), and

Figure 5. Pattern of hyperpolarization matches pattern of retraction temporally and spatially
Spread of spontaneous activity is greatest at E11.5 where it covers the entire surface of the hindbrain. Intensity of Ca^{2+} signal is greater at the midline compared with the lateral regions. The three sites of whole-cell patch clamp are shown as coloured circles. The propagation retracts laterally and medially at E13.5. Spontaneous activity disappears by E15.5. The × marks indicate hyperpolarization of the resting membrane potential in cells recorded from the region, demonstrating the progressive regional (or spatial) exclusion from spontaneous waves caused by hyperpolarization.

retraction and disappearance of spontaneous activity may signal cessation of cell proliferation across the hindbrain.

It is also possible that the circuit is changing from a gap junction-based system to an adult form of neuronal communication: synaptic transmission. This transition may take time even after spontaneous activity disappears because the circuitry at E15.5 still seems to support propagation of events, as evidenced by the induction of events using high $[K^+]_o$ ACSF (Fig. 4). However, this propagation already appears to be independent of gap junctional coupling (Fig. 4*B*), which is required for synchronization at earlier stages (Hunt *et al.* 2006*a*). Data from the Allen Brain Atlas (http://www.brain-map.org) demonstrate that mRNAs encoding synaptic proteins such as syntaxin-1, synapsin I and the presynaptic $Ca_v2.1$ channel are detected in high levels starting on or after E15.5. In addition, a large number of glutamate receptors become upregulated at E15.5. Acute bath application of 2 μM AMPA can evoke propagating events along the midline of quiescent hindbrain at E14.5–E15.5 ($n = 5$, data not shown), but the activated glutamatergic receptors may include extrasynaptic sites. More work needs to be done to determine whether the mouse hindbrain support synaptic transmission at or after E15.5, coinciding with the cessation of spontaneous activity.

We have demonstrated that the spontaneous activity recorded in the E11.5 hindbrain undergoes a characteristic spatial and temporal retraction mediated by progressive hyperpolarization of the resting membrane potential and increase in resting conductance. The last region to undergo these changes is the InZ, which retains the ability to support events until relatively late in development. The fact that events can be induced in midline cells by membrane depolarization, and that resting membrane potential is more closely set by E_K than E_{Cl}, suggests that changes in expression of resting K^+ conductance may be crucial in the spatiotemporal regulation of spontaneous activity.

Proper development of neuronal circuits requires spontaneous activity, but as the circuits mature, the system needs to desynchronize activity to switch from widespread network propagation to local information processing. Reducing membrane excitability by hyperpolarization of the resting membrane potential and increasing resting conductance are effective mechanisms to desynchronize activity in a spatiotemporal manner, while allowing information processing to occur at the synaptic and cellular level. Since spontaneous activity raises $[Ca^{2+}]_i$, the retraction sequence itself may be regulated by gene expression. Calcium influx that results from spontaneous activity may upregulate expression of resting ion channels, suppressing subsequent Ca^{2+} influx by membrane hyperpolarization and increased resting conductance, effectively turning off spontaneous activity in a feedback loop. At the same time, the influx of Ca^{2+} may also upregulate synaptic proteins and prepare individual neurons to support synaptic transmission as the primary form of cellular communication.

References

Aller MI & Wisden W (2008). Changes in expression of some two-pore domain potassium channel genes (KCNK) in selected brain regions of developing mice. *Neuroscience* **151**, 1154–1172.

Bosma MM (2010). Timing and mechanism of a window of spontaneous activity in embryonic mouse hindbrain development. *Ann N Y Acad Sci* **1198**, 182–191.

Butts DA, Feller MB, Shatz CJ & Rokhsar DS (1999). Retinal waves are governed by collective network properties. *J Neurosci* **19**, 3580–3593.

Conhaim J, Easton CR, Becker MI, Barahimi M, Cedarbaum ER, Moore JG, Mather LF, Dabagh S, Minter DJ, Moen SP & Moody WJ (2011). Developmental changes in propagation patterns and transmitter dependence of waves of spontaneous activity in the mouse cerebral cortex. *J Physiol* **589**, 2529–2541.

Corlew R, Bosma MM & Moody WJ (2004). Spontaneous, synchronous electrical activity in neonatal mouse cortical neurones. *J Physiol* **560**, 377–390.

Flavell SW & Greenberg ME (2008). Signaling mechanisms linking neuronal activity to gene expression and plasticity of the nervous system. *Annu Rev Neurosci* **31**, 563–590.

Garaschuk O, Linn J, Eilers J & Konnerth A (2000). Large-scale oscillatory calcium waves in the immature cortex. *Nat Neurosci* **3**, 452–459.

Godfrey KB & Swindale NV (2007). Retinal wave behavior through activity-dependent refractory periods. *PLoS Comput Biol* **3**, e245.

Gust J, Wright JJ, Pratt EB & Bosma MM (2003). Development of synchronized activity of cranial motor neurons in the segmented embryonic mouse hindbrain. *J Physiol* **550**, 123–133.

Hanson MG, Milner LD & Landmesser LT (2008). Spontaneous rhythmic activity in early chick spinal cord influences distinct motor axon pathfinding decisions. *Brain Res Rev* **57**, 77–85.

Hennig MH, Adams C, Willshaw D & Sernagor E (2009). Early-stage waves in the retinal network emerge close to a critical state transition between local and global functional connectivity. *J Neurosci* **29**, 1077–1086.

Hille B (2001). *Ion Channels of Excitable Membranes*, 3rd edn. Sinauer Associates Inc.

Hughes SM, Easton CR & Bosma MM (2009). Properties and mechanisms of spontaneous activity in the embryonic chick hindbrain. *Dev Neurobiol* **69**, 477–490.

Hunt PN, McCabe AK & Bosma MM (2005). Midline serotonergic neurones contribute to widespread synchronized activity in embryonic mouse hindbrain. *J Physiol* **566**, 807–819.

Hunt PN, Gust J, McCabe AK & Bosma MM (2006*a*). Primary role of the serotonergic midline system in synchronized spontaneous activity during development of the embryonic mouse hindbrain. *J Neurobiol* **66**, 1239–1252.

Hunt PN, McCabe AK, Gust J & Bosma MM (2006*b*). Spatial restriction of spontaneous activity towards the rostral primary initiating zone during development of the embryonic mouse hindbrain. *J Neurobiol* **66**, 1225–1238.

Meister M, Wong RO, Baylor DA & Shatz CJ (1991). Synchronous bursts of action potentials in ganglion cells of the developing mammalian retina. *Science* **252**, 939–943.

Momose-Sato Y, Nakamori T & Sato K (2012*a*). Spontaneous depolarization wave in the mouse embryo: origin and large-scale propagation over the CNS identified with voltage-sensitive dye imaging. *Eur J Neurosci* **35**, 1230–1241.

Momose-Sato Y, Nakamori T & Sato K (2012*b*). Pharmacological mechanisms underlying switching from the large-scale depolarization wave to segregated activity in the mouse central nervous system. *Eur J Neurosci* **35**, 1242–1252.

Moody WJ & Bosma MM (2005). Ion channel development, spontaneous activity, and activity-dependent development in nerve and muscle cells. *Physiol Rev* **85**, 883–941.

Mooney R, Penn AA, Gallego R & Shatz CJ (1996). Thalamic relay of spontaneous retinal activity prior to vision. *Neuron* **17**, 863–874.

Moruzzi AM, Abedini NC, Hansen MA, Olson JE & Bosma MM (2009). Differential expression of membrane conductances underlies spontaneous event initiation by rostral midline neurons in the embryonic mouse hindbrain. *J Physiol* **587**, 5081–5093.

O'Donovan MJ, Chub N & Wenner P (1998). Mechanisms of spontaneous activity in developing spinal networks. *J Neurobiol* **37**, 131–145.

Rockhill W, Kirkman JL & Bosma MM (2009). Spontaneous activity in the developing mouse midbrain driven by an external pacemaker. *Dev Neurobiol* **69**, 689–704.

Roerig B & Feller MB (2000). Neurotransmitters and gap junctions in developing neural circuits. *Brain Res Brain Res Rev* **32**, 86–114.

Spitzer NC (2006). Electrical activity in early neuronal development. *Nature* **444**, 707–712.

Wang S, Polo-Parada L & Landmesser LT (2009). Characterization of rhythmic Ca^{2+} transients in early embryonic chick motoneurons: Ca^{2+} sources and effects of altered activation of transmitter receptors. *J Neurosci* **29**, 15232–15244.

Weissman TA, Riquelme PA, Ivic L, Flint AC & Kriegstein AR (2004). Calcium waves propagate through radial glial cells and modulate proliferation in the developing neocortex. *Neuron* **43**, 647–661.

Author contributions

Conception and design of the experiments: H.W., A.J.T. and M.M.B. Collection, analysis and interpretation of data: H.W., A.J.T. and M.M.B. Drafting the article or revising it critically for important intellectual content: H.W. and M.M.B. All authors approved the final version.

Acknowledgements

Special thanks to Bess Navarrete, Mark Shi, Lucy Liu, Bethanny Danskin, Veronica Rodriguez, Ashley Lin and Joseph Bosma-Moody for technical assistance, and to Bill Moody for critical reading of the manuscript. This work is supported by the National Science Foundation (NSF) IOS 0952395.